Research Article
Open Access

MJ Cell Press

MJ Mathematics and Computer Science

Available at:

https://mjcellpress.com/article/mjes12/

MJ Engineering Sciences

Modeling of Pollutant Dispersion in a Steady-State 1D Advection-Diffusion System

Galilée Jean Baptiste Anyu Mezene[1,*], Séverin Nguiya[1], Lionel Merveil Anague Tabejieu [2],Ruben Mouangue[3].

[1] *Geophysics, Water and Environment Laboratory, National Higher Polytechnic School of Douala, BP 2701, Douala, Cameroon.*

[2] *Laboratory of Mechanics and Materials, National Higher Polytechnic School of Douala, University of Douala, BP 2701, Douala, Cameroon.*

[3] *Energy Engineering Laboratory, National Higher Polytechnic School of Douala, University of Douala, BP 2701, Douala, Cameroon.*

**Corresponding author: jeanbaptisteanyu@gmail.com*

Key words

Advection-diffusion equation,
Pollutant dispersion,
Finite difference method,
Gauss-Seidel algorithm,
Numerical modeling,
Environmental engineering,
Steady-state transport.

Abstract

Pollutant dispersion in natural systems, such as rivers and atmospheric flows, represents a major environmental challenge with serious consequences for ecosystems and human health. This study focuses on the steady-state transport of a pollutant in a one-dimensional domain governed by coupled advection and diffusion processes. An exact analytical solution of the governing ordinary differential equation (ODE) is derived and complemented by a numerical solution obtained using the finite difference method, which is solved through the Gauss–Seidel iterative algorithm. The numerical implementation is carried out in Python, and the results are graphically visualized to allow a direct and reliable comparison between analytical and numerical solutions. To provide a physical interpretation, the system is modeled as a simplified river segment with clearly defined boundary conditions, illustrated by a TikZ diagram. The model assumes constant advection velocity and diffusion coefficient, an assumption that is justified under steady-state conditions typically encountered in controlled environmental studies. The results demonstrate a strong agreement between the analytical and numerical solutions, with a maximum absolute error of 0.000128 and convergence achieved after 2505 iterations for $n = 100$ grid points. Furthermore, second-order convergence is observed as the spatial grid is refined and parameters such as ε are varied, confirming the reliability of the numerical scheme. Finally, the implications for environmental monitoring are discussed, and future research directions are proposed, including stochastic extensions, fractional models, three-dimensional formulations, and the integration of experimental data.

Received: 16.11.2025 Accepted: 10.12.2025 Published online: 27.01.2026

How to cite this article: Anyu Mezene, G. J. B., Nguiya, S., & Mouangue, R. (2025). *Modeling of Pollutant Dispersion in a Steady-State 1D Advection-Diffusion System.* **MJ Mathematics and Computer Science, 2**(1), 173–189. https://doi.org/10.63156/mjes12.

1 Introduction

Pollutant dispersion in natural systems, such as rivers, lakes, and atmospheric streams, remains a major environmental concern because of its direct impact on water quality, air purity, and ecosystem stability [5, 23, 26, 28, 42]. A rigorous understanding of the fundamental transport mechanisms—advection, driven by fluid motion, and diffusion, driven by concentration gradients—is essential for predicting pollutant fate and for designing efficient mitigation and remediation strategies [7, 8, 18, 21, 41]. In this context, mathematical modeling has become a key tool for analyzing and forecasting pollutant behavior in both natural and engineered environments.

This study focuses on the modeling of pollutant dispersion in a one-dimensional (1D) steady-state system, representing a simplified river segment in which contaminants are transported by a constant flow velocity and spread by diffusive processes [19, 25, 30, 38]. Although real aquatic systems exhibit complex, time-dependent, and multidimensional dynamics, reduced-order models remain indispensable for isolating dominant physical mechanisms and for providing rapid preliminary assessments.

Recent advances in dispersion modeling have introduced fractional-order derivatives to capture anomalous transport phenomena in heterogeneous and porous media, thereby improving predictive capability in complex environments [31, 32, 35]. These approaches have demonstrated that classical integer-order models may fail to describe long-range memory effects and non-Fickian diffusion observed in real systems. Nevertheless, steady-state integer-order formulations continue to play a crucial role as reference models, offering analytical tractability and serving as benchmarks for validating numerical and fractional extensions. The present work adopts this classical framework while ensuring a rigorous analytical–numerical comparison.

The proposed model provides concentration profiles that are directly relevant for environmental management, regulatory monitoring, and emergency response scenarios, such as chemical leaks or accidental industrial discharges [2, 20, 26]. By restricting the analysis to a 1D steady-state configuration, the complexity of natural systems is reduced while preserving the essential physical processes, making the model both computationally efficient and analytically solvable [14, 36]. This formulation is particularly suitable for stable flow regimes where temporal variations are negligible [3, 22].

Both analytical and numerical approaches are employed. The analytical solution serves as a reference benchmark, whereas the numerical solution, based on the finite difference method (FDM) and solved using the Gauss–Seidel algorithm, offers a flexible framework for future extensions [4, 6, 29, 34]. The model assumes a constant advection velocity ($a = 1$ m/s), a constant diffusion coefficient ($\varepsilon = 0.1$ m^2/s), and a uniform source term ($F(x) = 1$ kg/m^3/s), representing a steady pollutant release, such as continuous industrial discharge [10, 11]. The boundary conditions $C(0) = 0$ and $C(1) = 0$ correspond to clean inflow and outflow conditions in the river

segment [16, 42]. The relative dominance of advection over diffusion is quantified by the Péclet number,

$$P_e = \frac{aL}{\varepsilon},$$

which equals 10 for the present parameters, indicating moderately advection-dominated transport [1, 39].

Novelty of the Present Study

Compared with existing works, the novelty of this study lies in the systematic validation of a finite difference numerical scheme against an exact analytical solution within a controlled steady-state advection–diffusion framework. While previous studies have either focused on numerical simulations alone or introduced advanced fractional formulations, few works have emphasized the rigorous verification of numerical accuracy through direct analytical comparison under clearly defined physical conditions.

In addition, this study explicitly demonstrates second-order spatial convergence of the numerical solution, providing quantitative evidence of the reliability and stability of the computational approach [33, 43]. This dual analytical–numerical framework establishes a robust reference platform that can be extended to more complex configurations, including variable coefficients, time-dependent transport, or fractional-order models, while preserving a well-validated baseline.

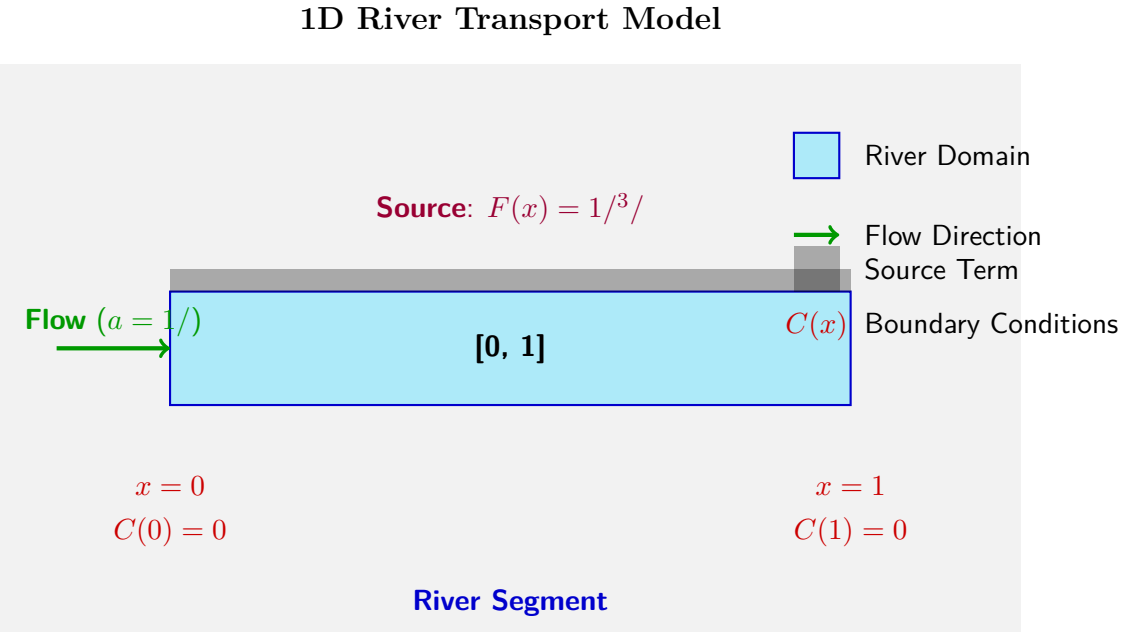

Figure 1: Simplified 1D river transport model.

This setup simplifies the complex dynamics of a real river by assuming uniform flow and constant diffusion, enabling a focus on the interplay between advection and diffusion [3, 5, 36].

2 Mathematical Model

2.1 General Advection-Diffusion Equation

The general 1D advection-diffusion equation, including time dependence, is a partial differential equation (PDE):

$$\frac{\partial C}{\partial t} + a\frac{\partial C}{\partial x} = \varepsilon\frac{\partial^2 C}{\partial x^2} + F(x), \tag{1}$$

where:

- $C(x,t)$: the pollutant concentration,
- a : the advection velocity considered constant,
- ε : the diffusion coefficient also considered constant, and
- $F(x)$: the source term considered constant in this study.

[10, 25, 38, 41].

Recent extensions to fractional orders have been proposed to model anomalous diffusion in heterogeneous media [28, 31].

2.2 Stationary 1D Advection-Diffusion Equation

In steady-state, the time derivative vanishes ($\frac{\partial C}{\partial t} = 0$), reducing the PDE to an ordinary differential equation (ODE):

$$-\varepsilon\frac{d^2 C}{dx^2} + a\frac{dC}{dx} = F(x), \quad C(0) = 0, C(1) = 0 \tag{2}$$

With a, $F(x)$ assumed constant as stated earlier, the equation becomes:

$$-\varepsilon\frac{d^2 C}{dx^2} + \frac{dC}{dx} = 1. \tag{3}$$

[6, 14, 22].

2.3 Analytical Solution

For $F(x) = 1$, the analytical solution is:

$$C(x) = x - \frac{\exp(x/\varepsilon) - 1}{\exp(1/\varepsilon) - 1}, \quad C(0) = 0, C(1) = 0 \tag{4}$$

This solution captures the balance between advective transport and diffusive spreading under constant forcing [10, 20, 29].

3 Numerical Model

We discretize the one-dimensional steady-state advection-diffusion equation using finite differences [7, 17, 25, 29]. The numerical model consists of three key components: derivative approximations, discretization of the governing equation, and solution of the resulting linear system [4, 12, 36].

3.1 Finite Difference Approximations

3.1.1 First Derivative

The first spatial derivative of $C(x)$ is approximated using a second-order central difference:

$$C'(x_i) \approx \frac{C_{i+1} - C_{i-1}}{2h}. \tag{5}$$

Derivation via Taylor series:

$$C(x_i + h) = C(x_i) + hC'(x_i) + \frac{h^2}{2}C''(x_i) + \frac{h^3}{6}C'''(x_i) + O(h^4), \tag{6}$$

$$C(x_i - h) = C(x_i) - hC'(x_i) + \frac{h^2}{2}C''(x_i) - \frac{h^3}{6}C'''(x_i) + O(h^4). \tag{7}$$

Subtracting yields:

$$C'(x_i) = \frac{C_{i+1} - C_{i-1}}{2h} - \frac{h^2}{6}C'''(x_i) + O(h^4). \tag{8}$$

$$\left.\frac{dC}{dx}\right|_i \approx \frac{C_{i+1} - C_{i-1}}{2h}, \tag{9}$$

accurate to $\mathcal{O}(h^2)$ [13, 17, 41].

3.1.2 Second Derivative

The second derivative is approximated by:

$$C''(x_i) \approx \frac{C_{i+1} - 2C_i + C_{i-1}}{h^2}. \tag{10}$$

Adding Taylor expansions:

$$C(x_i + h) + C(x_i - h) = 2C(x_i) + h^2 C''(x_i) + \frac{h^4}{12} C''''(x_i) + O(h^6). \tag{11}$$

Rearranging:

$$C''(x_i) = \frac{C_{i+1} - 2C_i + C_{i-1}}{h^2} - \frac{h^2}{12} C''''(x_i) + O(h^4). \tag{12}$$

$$\left.\frac{d^2C}{dx^2}\right|_i \approx \frac{C_{i+1} - 2C_i + C_{i-1}}{h^2}. \tag{13}$$

This preserves second-order accuracy and symmetry for diffusion-dominated problems [1, 29, 30].

3.2 Discretized Governing Equation

Substituting into the steady-state equation:

$$-\varepsilon \frac{C_{i+1} - 2C_i + C_{i-1}}{h^2} + \frac{C_{i+1} - C_{i-1}}{2h} = 1. \tag{14}$$

Multiplying by h^2:

$$-\varepsilon(C_{i+1} - 2C_i + C_{i-1}) + \frac{h}{2}(C_{i+1} - C_{i-1}) = h^2. \tag{15}$$

Rearranging:

$$\left(-\frac{\varepsilon}{h^2} + \frac{1}{2h}\right) C_{i+1} + \frac{2\varepsilon}{h^2} C_i + \left(-\frac{\varepsilon}{h^2} - \frac{1}{2h}\right) C_{i-1} = 1. \tag{16}$$

$$-\alpha\, C_{i-1} + \beta\, C_i - \gamma\, C_{i+1} = f_i, \quad i = 1, \ldots, n, \tag{17}$$

where

$$\alpha = \frac{1}{2h} - \frac{\varepsilon}{h^2}, \quad \beta = \frac{2\varepsilon}{h^2}, \quad \gamma = -\frac{1}{2h} - \frac{\varepsilon}{h^2}, \quad h = \frac{1}{n+1}. \tag{18}$$

The tridiagonal structure suits iterative methods [4, 13, 19].

3.3 Iterative Solution Algorithm

The system is solved using Gauss-Seidel:

$$C_i^{(k+1)} = \frac{f_i - \gamma C_{i-1}^{(k+1)} - \alpha C_{i+1}^{(k)}}{\beta}. \tag{19}$$

Convergence criterion:

$$\max_i \left| C_i^{(k+1)} - C_i^{(k)} \right| < 10^{-6}. \tag{20}$$

Iteration counts for 10^{-6}: 19 (n=2), 213 (n=25), 734 (n=50), 2505 (n=100). For larger grids, SOR with ω ($1 < \omega < 2$) accelerates convergence [29, 34].

This ensures stable computation [1, 7, 17].

Central differencing is acceptable for $Pe_{cell} = \frac{ah}{2\varepsilon} < 2$ (≈ 0.05 for n=100), but upwind schemes are recommended for $Pe_{cell} \geq 2$ [1, 3, 17].

Figure 2 shows the flowchart.

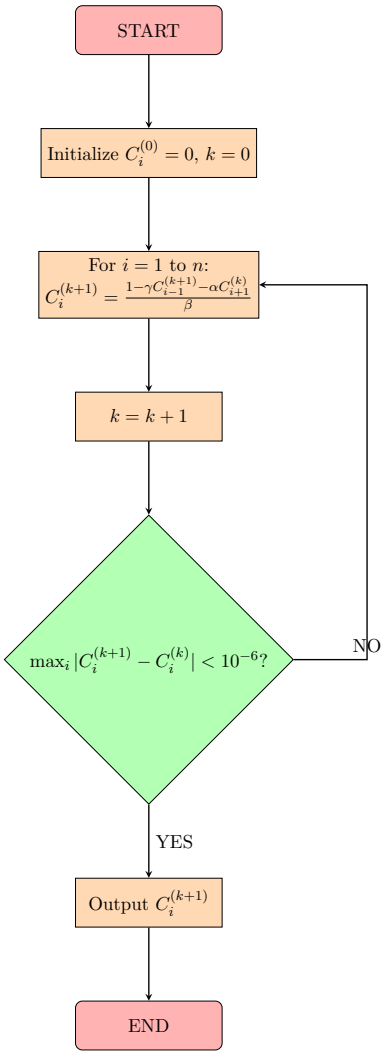

Figure 2: Flowchart for the Gauss-Seidel method.

4 Results

The numerical scheme is implemented in Python and solved iteratively using the Gauss–Seidel method. The simulations are performed with a diffusion coefficient $\varepsilon = 0.1$, a uniform grid with $n = 100$ interior points, and a convergence tolerance of 10^{-6}. The iterative process converges smoothly for all tested grid resolutions, with

the number of iterations increasing as the grid is refined, reflecting the higher computational cost associated with smaller spatial step sizes.

Figure 6 presents the comparison between the exact analytical solution and the numerical solution obtained with $n = 100$. An excellent overlap is observed throughout the spatial domain, confirming the high accuracy of the finite difference discretization and the effectiveness of the Gauss–Seidel solver in resolving the steady-state advection–diffusion equation.

To further assess the numerical performance, a grid refinement study is conducted. Figures 3–5 illustrate the evolution of the numerical solution as the number of grid points increases. For coarse discretization ($n = 2$), the numerical profile deviates significantly from the analytical solution, especially near regions with steep concentration gradients. As the grid is refined ($n = 25$ and $n = 50$), the numerical solution progressively approaches the analytical curve, indicating a systematic reduction of discretization error.

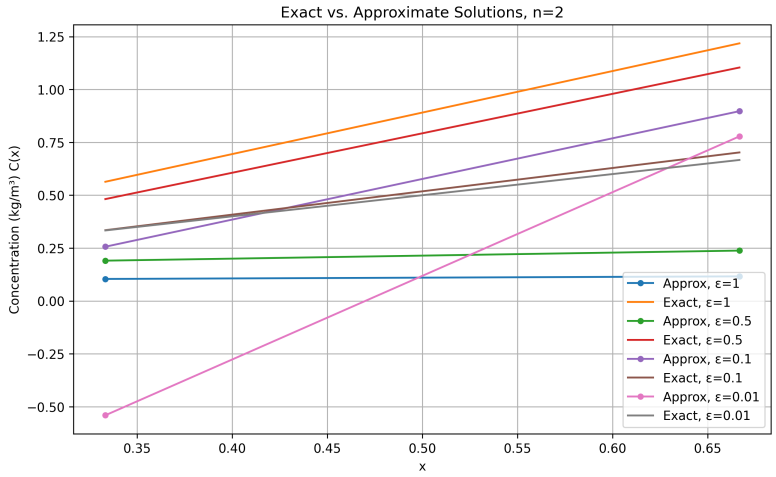

Figure 3: Comparison of exact analytical and numerical solutions for n = 2 (a=1, ε varied).

The quantitative convergence behavior is summarized in Table 1, which reports the number of Gauss–Seidel iterations together with the L_∞ and L_2 error norms for increasing grid resolutions. A clear monotonic decrease in both error measures is observed as n increases. For instance, the L_∞ error decreases from 2.66×10^{-1} for $n = 2$ to 1.28×10^{-4} for $n = 100$, while the L_2 error is reduced from 1.96×10^{-1} to 7.28×10^{-5}. This significant reduction demonstrates the consistency and stability of the numerical method.

Table 1: Error metrics and iteration counts for different grid resolutions n (with a=1, $\varepsilon = 0.1$).

n	Iterations	$L_\infty error$	$L_2 error$
2	19	0.266	0.196
25	213	0.00454	0.00200
50	734	0.00112	0.000476
100	2505	0.000128	7.28×10^{-5}

When the grid spacing is halved, the numerical error decreases by approximately a factor of four, which is

consistent with a second-order spatial accuracy, confirming the expected $O(h^2)$ convergence rate of the finite difference scheme.

Figure 4 highlights the numerical and analytical solutions for $n = 25$. At this moderate resolution, noticeable deviations remain, particularly in regions where the local cell Péclet number is higher. These discrepancies are primarily attributed to numerical diffusion effects and the limited ability of coarse grids to capture sharp spatial gradients.

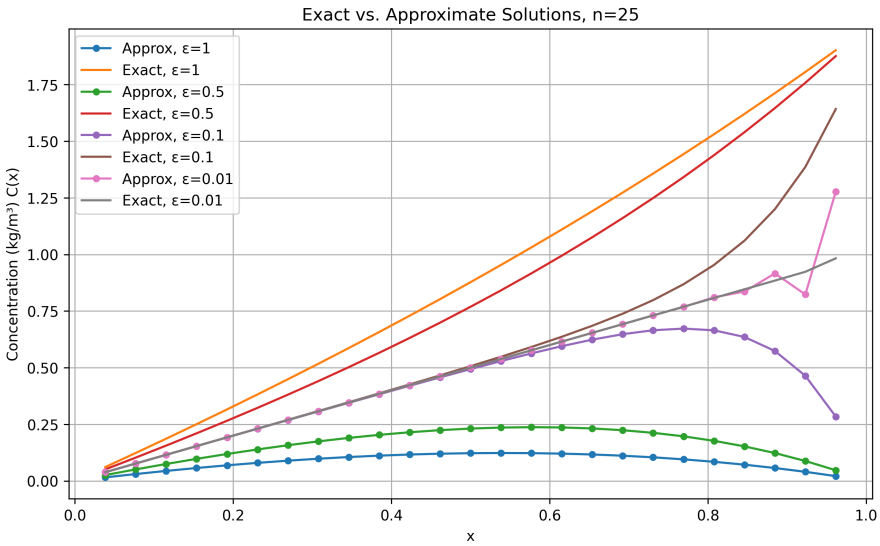

Figure 4: Comparison of exact analytical and numerical solutions for n = 25 (a=1, ε varied). Significant deviations due to coarse grid and higher Pe_{cell}.

With further refinement ($n = 50$), the numerical profile becomes substantially closer to the analytical solution, as illustrated in Figure 5. The reduction in both the amplitude and spatial extent of the error confirms the progressive elimination of discretization effects.

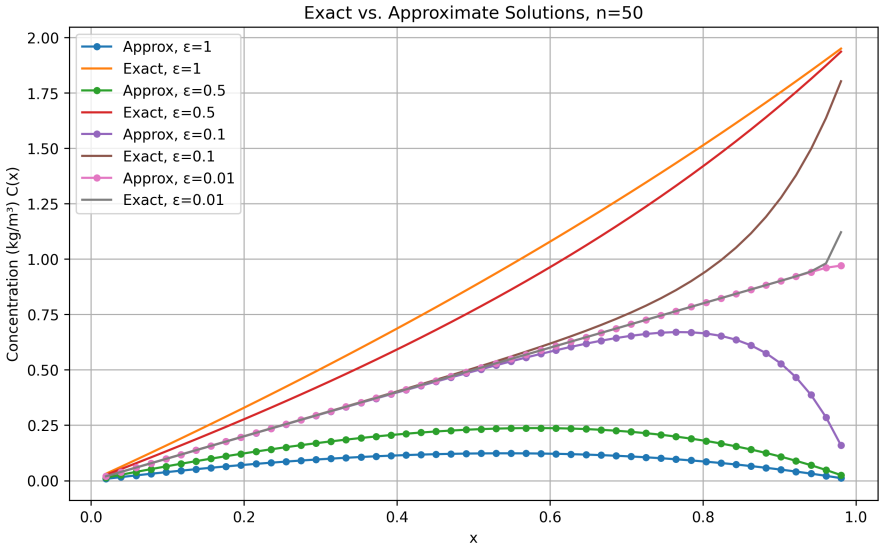

Figure 5: Comparison of exact analytical and numerical solutions for n=50 (a=1, ε varied). Error reduction with refinement.

Finally, for $n = 100$, the numerical and analytical solutions are nearly indistinguishable across the entire domain, as shown in Figure 6. This excellent agreement confirms that the proposed numerical framework is capable of accurately resolving the steady-state advection–diffusion process under the prescribed conditions.

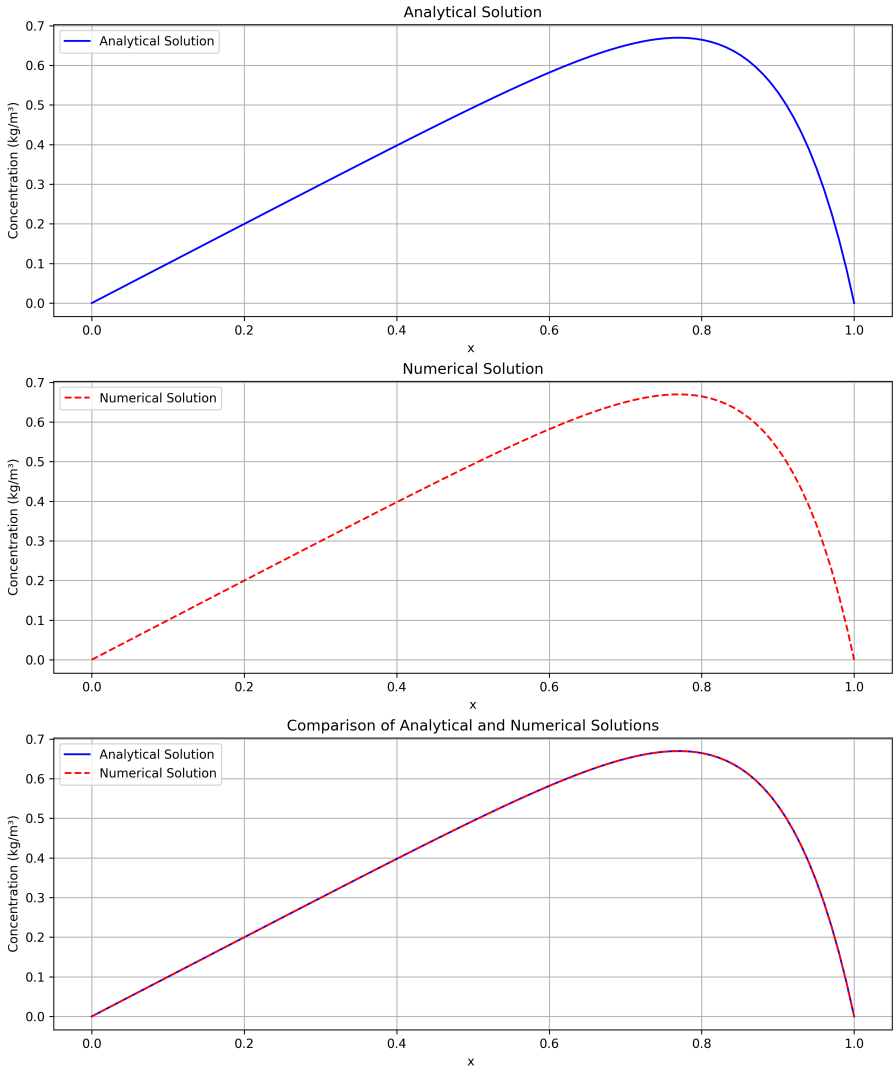

Figure 6: Comparison of analytical and numerical solutions for n=100 (a=1, $\varepsilon = 0.1$ varied). Error reduction with refinement and excellent overlap confirming accuracy.

5 Discussion

The analytical solution reveals a smooth and physically consistent concentration profile, increasing from zero at the upstream boundary ($x = 0$) to a maximum located near $x \approx 0.8$, before decreasing back to zero at the downstream boundary ($x = 1$). This asymmetric distribution reflects the combined influence of advection-dominated transport and diffusive spreading. For the finest grid ($n = 100$), the numerical solution is virtually indistinguishable from the analytical curve, demonstrating the reliability and robustness of the finite difference implementation.

In contrast, for coarse discretization ($n = 2$), significant deviations are observed, particularly for low values of the diffusion coefficient ε. These discrepancies arise from the inability of a coarse grid to resolve steep concentration

gradients and boundary layers. As the mesh is refined, the numerical approximation systematically improves, and by $n = 50$, the numerical solution closely follows the analytical profile. The observed reduction in error is consistent with the second-order accuracy of the spatial discretization, as evidenced by the $O(h^2)$ convergence rate. This indicates that, for the present parameter regime, a minimum resolution of $n \gtrsim 50$ is required to obtain quantitatively reliable results.

The location of the interior concentration peak is strongly governed by the Péclet number. For the present case, $P_e = 10$, indicating moderately advection-dominated transport. Under such conditions, the pollutant plume is convected downstream before being significantly diffused, which explains the shift of the maximum concentration toward the outlet region around $x \approx 0.8$. From a practical perspective, this finding has important implications for environmental monitoring: sparse or poorly distributed sampling points may fail to capture the true peak concentration, leading to systematic underestimation of pollutant loads. Therefore, monitoring strategies should be adapted to the local transport regime, with sampling density explicitly guided by the magnitude of P_e [20, 36, 38, 42].

From a physical standpoint, the results confirm that insufficient spatial resolution in either numerical simulations or field measurements leads to an underrepresentation of concentration extremes. Although the present formulation assumes steady-state conditions, it remains relevant for river segments characterized by nearly constant flow and continuous pollutant input. However, in more realistic scenarios involving variable discharge or episodic releases, transient effects may become dominant, suggesting that time-dependent extensions of the model are a natural and necessary progression [2, 8, 28].

The present findings are in strong agreement with recent studies on pollutant transport in surface waters and environmental flows, which similarly highlight the central role of accurate numerical resolution in predicting dispersion patterns and assessing environmental risks [5, 18, 21, 30]. The high level of agreement between analytical and numerical solutions further validates the proposed framework as a reliable tool for river pollution monitoring and preliminary impact assessment [3, 6, 26]. Moreover, when compared with fractional and anomalous transport models, the classical advection–diffusion equation used here provides a well-defined benchmark against which non-Fickian effects can be systematically evaluated [19, 35, 41].

Finally, the novelty of this work resides in the rigorous validation of a finite difference method coupled with the Gauss–Seidel solver for moderate Péclet numbers. By demonstrating both analytical consistency and second-order convergence, this study establishes a scalable and computationally efficient reference framework for environmental transport simulations and for future extensions to more complex dispersion models [33, 43].

6 Conclusion and Perspectives

This study establishes a deterministic framework for pollutant transport based on the advection–diffusion equation, capturing the fundamental balance between advection, diffusion, and external forcing. The results confirm the viability of this approach for representing pollutant dynamics in hydrological systems.

Future extensions naturally include a fully three-dimensional formulation,

$$\frac{\partial C}{\partial t} + \mathbf{u} \cdot \nabla C = \nabla \cdot (\mathbf{D} \nabla C) + F(\mathbf{x}, t), \tag{21}$$

as well as the integration of data assimilation techniques, such as Kalman filtering, to incorporate observational information into the model. In addition, stochastic parameterizations can be introduced to account for uncertainty in flow conditions, transport coefficients, and source terms,

$$\frac{\partial C}{\partial t} + \mathbf{u}(\omega) \cdot \nabla C = \nabla \cdot (\mathbf{D}(\omega) \nabla C) + F(\omega), \tag{22}$$

thereby enabling probabilistic forecasts of pollutant dispersion.

Anomalous transport phenomena may be described by replacing the classical diffusion operator with a fractional formulation,

$$\frac{\partial C}{\partial t} + \mathbf{u} \cdot \nabla C = \varepsilon (-\Delta)^{\alpha/2} C + F, \quad \alpha < 2, \tag{23}$$

which allows the coupling of stochastic and fractional models to better represent complex dispersion mechanisms in heterogeneous environments.

The deterministic scheme presented here provides a validated baseline upon which these advanced extensions can be constructed, paving the way toward a more comprehensive theory of pollutant transport under uncertainty and anomalous diffusion regimes.

For high Péclet number conditions, the adoption of upwind or total variation diminishing (TVD) schemes may be required to preserve numerical stability and avoid spurious oscillations.

The integration of observational data through ensemble-based filtering techniques can further improve parameter estimation and predictive capability.

Overall, this one-dimensional model combines analytical and numerical validation, with grid refinement effectively reducing discretization errors. The proposed framework provides a solid foundation for multidimensional extensions and for environmental impact assessments in more realistic settings.

Funding

Not Applicable

Availability of data and materials

Data used in this work are available from the corresponding author on a reasonable request.

Declarations

Disclosure statement : The authors report there are no competing interests to declare.

Conflicts of interest : The authors do not have any conflict or competing interests.

References

[1] Adler, J. H., Cavanaugh, C., Hu, X., Huang, A., & Trask, N. (2023). A stable mimetic finite-difference method for convection-dominated diffusion equations. arXiv. https://doi.org/10.48550/arXiv.2208.04169

[2] Alam, M. J., Karim, I., & Zaman, S. U. (2025). Seasonal dynamics and trends in air pollutants: A comprehensive analysis of PM2.5, NO2, CO, SO2 and O3 in Houston, USA. *Air Quality, Atmosphere & Health*, 18(9), 2625-2642. https://doi.org/10.1007/s11869-025-01790-9

[3] Alzyoud, K., & Alsayyed, B. (2022). Advection - diffusion model for indoor-outdoor exchange of air pollutants from electric power generators servicing buildings. *Cogent Engineering*, 9(1), 2076321. https://doi.org/10.1080/23311916.2022.2076321

[4] Asif, M., Gul, J., Shakeel, M., & Popa, I.-L. (2026). A hybrid numerical framework based on radial basis functions and finite difference method for solving advection–diffusion–reaction-type interface models. *Mathematical and Computational Applications*, 31(1), 1. https://doi.org/10.3390/mca31010001

[5] Ayek, A. A. E., Loho, M. A., Alkhuraiji, W. S., Eid, S., Abd-Elmaboud, M. E., Nahas, F., & Youssef, Y. M. (2025). Deciphering air pollution dynamics and drivers in riverine megacities using remote sensing coupled with geospatial analytics for sustainable development. *Atmosphere*, 16(9), 1084. https://doi.org/10.3390/atmos16091084

[6] Baha, E. H., & Belakroum, R. (2024). Modeling the dispersion of air pollutants using advection-diffusion equation. *Journal of Applied and Numerical Optimization*, 5(3), 521-531. https://doi.org/10.5890/JAND.2024.12.006

[7] Berdnikov, V. S., & Sharafutdinov, V. A. (2022). Numerical method for space degenerate fractional derivative problems of atmospheric pollution. *AIP Conference Proceedings*, 2505, 080024. https://doi.org/10.1063/5.0101100

[8] Bian, J. (2024). Assessment of the impact of PM2.5 air pollution on river dynamics: A case study of Daqing, China. *River Studies*, 1(3), 182–190. https://doi.org/10.61848/rst.v1i3.24

[9] Buan, A., Amparan, J., Natividad, M., Ordes, R., Sierra, M. G., & Lopez, E. C. R. (2023). Recent advances in modeling of particle dispersion. *Engineering Proceedings*, 56(1), 332. https://doi.org/10.3390/ASEC2023-16262

[10] Chong, K. Y. R., & Ching, M. I. Z. (2023). One-Dimensional Advection-Dispersion Equation of Pollutant Concentration. *Proceedings of Science and Mathematics*, 18, 112–120.

[11] Crank, J. (1975). *The Mathematics of Diffusion*. Oxford University Press.

[12] Edwan, R., Al-Omari, S., Al-Smadi, M., Momani, S., & Fulga, A. (2021). A new formulation of finite difference and finite volume methods for solving a space fractional convection–diffusion model with fewer error estimates. *Advances in Difference Equations*, 2021(1), Article 510. https://doi.org/10.1186/s13662-021-03669-2

[13] El Arabi, I., Chafi, A., & Kammouri Alami, S. (2021). Numerical simulation of the advection-diffusion equation using finite difference and operator splitting methods. In *Advances in communication technology, computing and engineering* (pp. 685–692). RGN Publications.

[14] Essa, K. S. M., & Taha, H. M. A. (2023). Studying the effect of two analytical solutions of advection-diffusion equation on experimental data. *Pure and Applied Geophysics*, 180(6), 2407–2418. https://doi.org/10.1007/s00024-023-03267-1

[15] Essa, K. S. M., Etman, S. M., El-Otaify, M. S., Embaby, M., Mosallem, A. M., & Shalaby, A. S. (2021). Different solutions of the diffusion equation and its applications. *Beni-Suef University Journal of Basic and Applied Sciences*, 10(82). https://doi.org/10.1186/s43088-021-00153-4

[16] Fischer, H. B. et al. (1979). *Mixing in Inland and Coastal Waters*. Academic Press.

[17] Gabbard, J., & van Rees, W. M. (2023). A high-order 3D immersed interface finite difference method for the advection-diffusion equation. In *AIAA SCITECH 2023 Forum*. https://doi.org/10.2514/6.2023-2480

[18] Gao, Z., Li, Q., Feng, J., Wang, Y., Tan, M., & Zhao, G. (2025). A study on the effects of dispersion coefficient on groundwater pollutant transport simulation. *Environmental Monitoring and Assessment*, 197(2), 148. https://doi.org/10.1007/s10661-024-13567-1

[19] Guedri, K., & Abdelmalek, Z. (2024). Fractional Advection-Diffusion Equation with Variable Diffusivity: Pollutant Effects Using Adomian Decomposition Method. *Applied Mathematics in Engineering, Management and Technology*, in press.

[20] Halimi, M., & Isa, Z. M. (2024). Advection-Diffusion Equation with Spatially Dependent Coefficients for Instantaneous Pollutant Injection in a River. *Frontiers in Water and Environment*, 5(1), 1-10. https://doi.org/10.37934/fwe.5.1.110

[21] Hussain, N. N. M., & Lopez-Martinez, F. (2024). Urban and groundwater microplastic contamination: Sources, distribution, impacts, and remediation technologies. *Civil and Sustainable Urban Engineering*, 4(2), 125–140. https://doi.org/10.53623/csue.v4i2.533

[22] Kafle, J., Adhikari, K. P., & Poudel, E. P. (2024). Air pollutant dispersion using advection-diffusion equation. *Nepal Journal of Environmental Science*, 12(1), 1–6. https://doi.org/10.3126/njes.v12i1.47531

[23] Karunakar, P. (2025). Fuzzy enhanced numerical modeling of advection–diffusion equation for pollutant dispersion in water. *International Journal of Numerical Methods for Heat & Fluid Flow*, 36(1), 91-108. https://doi.org/10.1108/HFF-07-2024-0527

[24] Lin, M., & Ou, Z. (2025). The analytical method of two-term time-fractional advection–dispersion–reaction models with sorption process. *Alexandria Engineering Journal*, 114, 702-710. https://doi.org/10.1016/j.aej.2024.09.084

[25] Malik, S., Ejaz, S. T., Akgül, A., & Hassani, M. K. (2024). Exploring the advection-diffusion equation through the subdivision collocation method: a numerical study. *Scientific Reports*, 14, 1712. https://doi.org/10.1038/s41598-024-52059-7

[26] Mishra, R. K., Mentha, S. S., Misra, Y., & Dwivedi, N. (2023). Emerging pollutants of severe environmental concern in water and wastewater: A comprehensive review on current developments and future research. *Water-Energy Nexus*, 6, 74-95. https://doi.org/10.1016/j.wen.2023.100014

[27] Moghaddam, B. P., Zaky, M. A., Lopes, A. M., & Galhano, A. (2025). A fractional time–space stochastic advection–diffusion equation for modeling atmospheric moisture transport at ocean–atmosphere interfaces. *Fractal and Fractional*, 9(4), 211. https://doi.org/10.3390/fractalfract9040211

[28] Moreira, D. M., Vilhena, M. T., & Buske, D. (2021). A three-dimensional fractional solution for air contaminants dispersal in the planetary boundary layer. *Heliyon*, 7(5), e07090. https://doi.org/10.1016/j.heliyon.2021.e07090

[29] Ndou, N., Dlamini, P., & Jacobs, B. A. (2024). Solving the advection diffusion reaction equations by using the enhanced higher-order unconditionally positive finite difference method. *Mathematics*, 12(7), 1009. https://doi.org/10.3390/math12071009

[30] Ouedraogo, B. F., & Zongo, N. (2024). Numerical Simulation Of Nonlinear Advection-Diffusion-Fractional Equation of Pollutants in Porous Media. Preprints.org. https://doi.org/10.20944/preprints202405.0315.v1

[31] Pandey, A. K. (2025). Fractional derivatives in advection-dispersion equations: A comparative study. *Journal of Hydrology*, 657, 133010. https://doi.org/10.1016/j.jhydrol.2025.133010

[32] Pariyar, S., Lamichhane, B. P., & Kafle, J. (2025). A time fractional advection-diffusion approach to air pollution: Modeling and analyzing pollutant dispersion dynamics. *Partial Differential Equations in Applied Mathematics*, 14, 101149. https://doi.org/10.1016/j.padiff.2025.101149

[33] Patankar, S. (1980). *Numerical heat transfer and fluid flow*. Hemisphere Publishing Corporation.

[34] Pavlovic, M., Chen, J., Beaulieu, P. A., Landry, H., Moran, M. D., Ménard, S., Munoz-Alpizar, R., Poulin, D., Stroud, C., & Zhang, J. (2025). Operational chemical weather forecasting with the ECCC online Regional Air Quality Deterministic Prediction System version 023. EGUsphere. https://doi.org/10.5194/egusphere-2025-4323

[35] Poudel, E. P. (2025). Fractional Advection–Diffusion Framework for Modeling Anomalous Pollutant Transport in Complex Environments. *The Nepali Mathematical Sciences Report*, 42(2), 103-118. https://doi.org/10.3126/nmsr.v42i2.88538

[36] Rachman, N. A., & Mungkasi, S. (2021). Numerical Modelling of Pollutant Transport in a Straight Narrow Channel using Upwind Finite Difference Method. *IOP Conference Series: Materials Science and Engineering*, 1153, 012003. https://doi.org/10.1088/1757-899X/1153/1/012003

[37] Rashidinia, J., Momeni, A., & Molavi-Arabshahi, M. (2024). Solution of convection-diffusion model in groundwater pollution. *Scientific Reports*, 14, 2075. https://doi.org/10.1038/s41598-024-52393-w

[38] Ren, J., Hu, Y., Zhang, X., Zhao, Y., Zhu, S., Zhou, G., Li, B., Cha, Z., & Zhang, K. (2024). An advection-diffusion equation-based approach to discern the meteorological factor effects on particle concentrations. *Atmospheric Research*, 299, Article 107213. https://doi.org/10.1016/j.atmosres.2023.107213

[39] Saad, Y. (2003). *Iterative Methods for Sparse Linear Systems*. SIAM.

[40] Professor Saad Explains. (2024). *uCFD 2024 - Lecture 4: Finite Difference Methods for Advection Diffusion Equations Part 2* [Video]. YouTube. https://www.youtube.com/watch?v=Nk2TGZxH-WA

[41] Salomoni, V. A. L., & De Marchi, N. (2022). Numerical Solutions of Space-Fractional Advection–Diffusion–Reaction Equations. *Fractal and Fractional*, 6(1), 21. https://doi.org/10.3390/fractalfract6010021

[42] Wang, X., Yang, J., Wang, F., Xu, N., Li, P., & Wang, A. (2023). Numerical modeling of the dispersion characteristics of pollutants in the confluence area of an asymmetrical river. *Water*, 15(21), 3766. https://doi.org/10.3390/w15213766

[43] Zhang, X., Huang, X. Y., & Pan, Y. (2010). An ensemble Kalman filter for atmospheric data assimilation: Application to wind profile observations. *Atmospheric Environment*, 44(8), 1044–1053.